Inorganic Chemistry
Article

Inorg. Chem. **2009,** *48,* 5027–5038 **5027**
DOI:10.1021/ic9002093

Alkylation of a Dimolybdenum SO Bridge, Subsequent Reactions, and Characterization of the Thioperoxide Bridge

Chi MinhTuong,[†] Whitney K. Hammons,[†] Ashley L. Howarth,[†] Kelly E. Lutz,[†] Ackim D. Maduvu,[†] Laura B. Haysley,[†] Brian R. T. Allred,[†] Lenore K. Hoyt,[†,‡] Mark S. Mashuta,[†] and Mark E. Noble*[,†]

[†]*Department of Chemistry, University of Louisville, Louisville, Kentucky 40292, and* [‡]*Department of Chemistry, Idaho State University, Pocatello, Idaho 83209*

Received February 2, 2009

The SO bridge of the complex, $[Mo_2(NTo)_2(S_2P(OEt)_2)_2(\mu\text{-}O_2CMe)(\mu\text{-}SBn)(\mu\text{-}SO)]$, **1**, displayed nucleophilicity at O, giving alkylation products $[Mo_2(NTo)_2(S_2P(OEt)_2)_2(\mu\text{-}O_2CMe)(\mu\text{-}SBn)(\mu\text{-}SOR)]^+$, **4**$^+$, which contained the thioperoxide bridge. These cations were then subject to nucleophilic attack by two pathways. Debenzylation of the bridge thiolate in **4**$^+$ afforded neutral $[Mo_2(NTo)_2(S_2P(OEt)_2)_2(\mu\text{-}O_2CMe)(\mu\text{-}S)(\mu\text{-}SOR)]$, **5**; de-esterification of a dithiophosphate ligand in **4**$^+$ gave $[Mo_2(NTo)_2(S_2P(=O)(OEt))(S_2P(OEt)_2)(\mu\text{-}O_2CMe)(\mu\text{-}SBn)(\mu\text{-}SO)]$, **6**, which contained a monoester, dithiophosphate ligand. Complex **1** gave a slow and clean reaction in the crystalline state, further demonstrating its nucleophilicity by attacking a neighboring molecule in its lattice. X-ray crystallography confirmed the thioperoxide linkage and revealed structural similarities of the $Mo_2(\mu\text{-}SOR)$ unit to sulfenate esters (RSOR) and related derivatives.

Introduction

Sulfur is one of the most interdisciplinary of all elements, impacting an extensive range of biological, atmospheric, geochemical, and cosmochemical natural processes, in addition to human societal and industrial processes. Within the scope of the general chemistry of sulfur, sulfur/oxygen compounds are among the most common and among the most important, thus endowing the study of S/O functional units with tremendous importance. The simplest S_1O_1 unit traverses the entire range of main group, transition metal, and organic chemistry, including biochemical applications therein. This fundamental SO unit appears at its simplest as diatomic SO itself, a fleeting molecule at earthly conditions but which nonetheless does have an astronomical presence.[1] The SO unit appears far more extensively in a variety of compounds including thionyls, sulfoxides, sulfenic acids and esters, sulfines, and numerous metallovariants and complexes of these.

Organic sulfoxides, $R_2S{=}O$, are among the most numerous compounds which contain the S_1O_1 unit. While metal complexes containing molecular sulfoxide ligands are very well-known,[2−4] metallovariants of sulfoxides are the present emphasis. These have long been considered[5−7] to include SO-bridged species structurally represented as $M_2(\mu\text{-}S{=}O)$, as well as sulfinyl−metal complexes represented by $MS(=O)$-R. Sulfinyl ligands (S-bound, $-S(=O)R$) have been known for some time[8] and continue to attract considerable attention, spurred in large part by biological applications.[9−11] Their complexes are often referred to as sulfenate systems, but this term can be problematic since the general bonding modes are not of classical "sulfenate" character. (Unfortunately, the terminology has become inconsistent between inorganic and organic usage of these terms and those of related systems.) In this report, $-S(=O)R$ ligands will be termed sulfinyl ligands, by direct analogy to acyl (C-bound, $-C(=O)R$) ligands; in this manner, $-S(=O)R$ is clearly distinguished from sulfenate (thioperoxide) and other classical "sulfenyl" (X-SR) characters. The consideration of $MS(=O)R$ as a sulfoxide analog rather than as a complex containing a sulfenate ion can more readily account for various properties and for the stabilization of the RSO^- moiety upon binding to a metal via S.

* To whom correspondence should be addressed. E-mail: menoble@louisville.edu.

(1) Tennyson, J. In *Handbook of Molecular Physics and Quantum Chemistry*; Wilson, S., Ed.; John Wiley & Sons: Chichester, U.K., 2003; pp 1−14. Herbst, E. *Annu. Rev. Phys. Chem.* **1995**, *46*, 27–53.
(2) Calligaris, M. *Coord. Chem. Rev.* **2004**, *248*, 351–375. Calligaris, M.; Carugo, O. *Coord. Chem. Rev.* **1996**, *153*, 83–154.
(3) Alessio, E. *Chem. Rev.* **2004**, *104*, 4203–4242.
(4) Kukushkin, V. Y. *Coord. Chem. Rev.* **1995**, *139*, 375–407.
(5) Jackson, W. G.; Sargeson, A. M. In *Rearrangements in Ground and Excited States*; de Mayo, P., Ed.; Academic Press: New York, 1980; Vol. 2, pp 273−378.
(6) Besenyei, G.; Lee, C.-L.; Gulinski, J.; Rettig, S. J.; James, B. R.; Nelson, D. A.; Lilga, M. A. *Inorg. Chem.* **1987**, *26*, 3622–3628.
(7) Lorenz, I.-P.; Messelhäuser, J.; Hiller, W.; Conrad, M. *J. Organomet. Chem.* **1986**, *316*, 121–138.
(8) George, T. A.; Watkins, D. D. *Inorg. Chem.* **1973**, *12*, 398–402.
(9) Weigand, W.; Wünsch, R. *Chem. Ber.* **1996**, *129*, 1409–1419.
(10) Grapperhaus, C. A.; Darensbourg, M. Y. *Acc. Chem. Res.* **1998**, *31*, 451–459.
(11) Kovacs, J. A. *Chem. Rev.* **2004**, *104*, 825–848.

Published on Web 4/28/2009

While several dimetal sulfoxide analogs, $M_2(\mu\text{-SO})$, are known, their numbers, along with those of SO-bridged complexes of any nuclearity, M_xSO,[12−19] pale in comparison to the number of metal−SO_2 complexes whose synthesis and reactivity have been extensively well-developed.[12,20,21] A major reason for the disparity in the studies of SO and SO_2 ligand systems is the difficulty of preparation. Due to the fleeting existence of SO, it is not a simple task to combine free SO with a metal complex, although precursors containing an SO equivalent are sometimes used. Dimeric $M_2(\mu\text{-SO})$ complexes are sometimes accessible via oxygenation of a bridge sulfide, $M_2(\mu\text{-S})$, but these can be hard to control since there is a facile tendency toward overoxidation to SO_2-bridged products, $M_2(\mu\text{-SO}_2)$. Among the known $M_2(\mu\text{-SO})$ compounds, there are a few structural variations,[4,22] but the emphasis herein will be on those which have η^1-SO and pyramidal sulfur, and which therefore have some structural analogy to sulfoxides.

Compared to organic sulfoxides, $R_2S{=}O$, the isomeric sulfenate esters, RS−OR, are less common, partly due to their more reactive nature. Sulfoxide/sulfenate ester isomerizations have been of considerable interest for some time, and both directions are known.[23,24] Sulfenate esters are well-known members of the general family of sulfenyl derivatives which also includes sulfenic acids, sulfenamides, sulfenimines, sulfenyl halides, and disulfides.[25−27] Sulfenate esters are thioperoxides, and RSOR can be compared to peroxides ROOR and also to persulfides RSSR.

Relative to organic derivatives, there are few isolable metallosulfenate ester analogs in any of the various forms, such as MS−OM, MS−OR,[28] or RS−OM,[29,30] although the latter may be the simple salt form for sulfenate anions.[31] Metal complexes with molecular sulfenate esters, RSOR, as ligands have also been reported.[32,33]

In light of the importance and the extensive chemistry of the SO functional group in nonmetal systems, there is considerable potential for the SO group in dimetal systems. Studies of the reactivity of the SO bridge in the $Mo_2(\mu\text{-SO})$ complex, $[Mo_2(NTo)_2(S_2P(OEt)_2)_2(\mu\text{-}O_2CMe)(\mu\text{-SBn})(\mu\text{-SO})]$, **1**, have thus been undertaken. (To = *p*-tolyl; Bn = benzyl; other abbreviations are common.) The present report describes nucleophilic behavior leading to *O*-alkylation and the formation of the thioperoxide ligand, ROS^-. This nucleophilicity manifests in solution and even in the crystal phase, the latter providing an interesting and clean solid-state reaction of **1**. Additional solution reactions are also presented, including the formation of a dimolybdenum sulfenate ester analog.

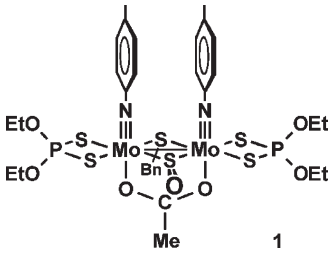

1

Results

For simplicity, the dimolybdenum derivatives of general formula $[Mo_2(NTo)_2(S_2P(OEt)_2)_2(\mu\text{-}O_2CMe)(\mu\text{-SR})(\mu\text{-SZ})]$ will be represented by several abbreviations. The simple bracket notation $\{Mo_2\}$ will denote the bis(*p*-tolylimido)-bis(diethyl dithiophosphato)-μ-acetato-dimolybdenum(V) basic framework, $\{Mo_2(NTo)_2(S_2P(OEt)_2)_2(\mu\text{-}O_2CMe)\}^{3+}$. Prefixed and suffixed to this $\{Mo_2\}$ bracket term will be the μ-S bridges, along with their functional groups as appropriate. By this notation, the dimolybdenum sulfoxide $[Mo_2(NTo)_2(S_2P(OEt)_2)_2(\mu\text{-}O_2CMe)(\mu\text{-SBn})(\mu\text{-SO})]$, **1**, is written as $BnS\{Mo_2\}SO$. The artwork is also simplified: rotation of the broadside view above and truncation of ancillary ligands gives the simplified stick diagram illustrated below.

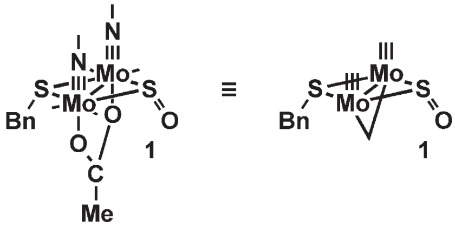

The corresponding sulfide and μ-SO_2 complexes are given by $BnS\{Mo_2\}S$, **2**, and $BnS\{Mo_2\}SO_2$, **3**.

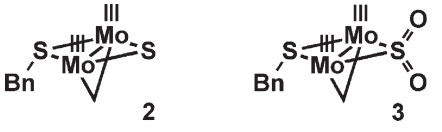

(12) Schenk, W. A. *Angew. Chem., Int. Ed. Engl.* **1987**, *26*, 98–109.
(13) Pandey, K. K. *Prog. Inorg. Chem.* **1992**, *40*, 445–502.
(14) Gong, J. K.; Fanwick, P. E.; Kubiak, C. P. *J. Chem. Soc., Chem. Commun.* **1990**, 1190–1191.
(15) Heyke, O.; Hiller, W.; Lorenz, I.-P. *Chem. Ber.* **1991**, *124*, 2217–2222.
(16) Karet, G. B.; Stern, C. L.; Norton, D. M.; Shriver, D. F. *J. Am. Chem. Soc.* **1993**, *115*, 9979–9985.
(17) Wang, R.; Mashuta, M. S.; Richardson, J. F.; Noble, M. E. *Inorg. Chem.* **1996**, *35*, 3022–3030.
(18) Huang, R.; Guzei, I. A.; Espenson, J. H. *Organometallics* **1999**, *18*, 5420–5422.
(19) Böttcher, H.-C.; Graf, M.; Merzweiler, K.; Wagner, C. *Inorg. Chim. Acta* **2003**, *350*, 399–406.
(20) Ryan, R. R.; Kubas, G. J.; Moody, D. C.; Eller, P. G. *Struct. Bonding (Berlin)* **1981**, *46*, 47–100.
(21) Kubas, G. J. *Acc. Chem. Res.* **1994**, *27*, 183–190.
(22) Bianchini, C.; Mealli, C.; Meli, A.; Sabat, M. *J. Chem. Soc., Chem. Commun.* **1985**, 1024–1025.
(23) Braverman, S. In *The Chemistry of Sulphenic Acids and Derivatives*; Patai, S., Ed.; John Wiley & Sons: Chichester, U.K., 1990; pp 311−359. Braverman, S. In *The Chemistry of Sulphones and Sulphoxides*; Patai, S., Rappoport, Z., Stirling, C. J. M., Eds.; John Wiley & Sons: Chichester, U.K., 1988; pp 717−757.
(24) Amaudrut, J.; Wiest, O. *J. Am. Chem. Soc.* **2000**, *122*, 3367–3374. Tureček, F. *J. Phys. Chem. A* **1998**, *102*, 4703–4713.
(25) Patai, S. *The Chemistry of Sulphenic Acids and Derivatives*; John Wiley & Sons: Chichester, U.K., 1990.
(26) Hogg, D. R. In *Comprehensive Organic Chemistry*; Jones, D. N., Ed.; Pergamon Press: Oxford, U.K., 1979; Vol. 3, pp 261−310.
(27) Kühle, E. *Synthesis* **1971**, 617–638.
(28) Hoots, J. E.; Rauchfuss, T. B.; Wilson, S. R. *J. Chem. Soc., Chem. Commun.* **1983**, 1226–1228.
(29) Jackson, W. G.; Rahman, A. F. M. M. *Inorg. Chem.* **2003**, *42* 383–388.
(30) For related variants, see: Ng, S.; Ziller, J. W.; Farmer, P. J. *Inorg. Chem.* **2004**, *43*, 8301–8309. Eremenko, I. L.; Berke, H.; Kolobkov, B. I.; Novotortsev, V. M. *Organometallics* **1994**, *13*, 244–252.
(31) O'Donnell, J. S.; Schwan, A. L. *J. Sulfur Chem.* **2004**, *25*, 183–211.
(32) Steudel, R.; Kustos, M.; Schmidt, H.; Wenschuh, E.; Kersten, M.; Wloszczynski, A. *J. Chem. Soc., Dalton Trans.* **1994**, 2509–2513.
(33) Kuhnert, N.; Burzlaff, N.; Dombrowski, E.; Schenk, W. A. *Z. Naturforsch.* **2002**, *57B*, 259–274.

BnS{Mo_2}SO, **1**, had been previously prepared[17] by oxygenation of the sulfide bridge of BnS{Mo_2}S, **2**, using *m*-chloroperbenzoic acid in CH_2Cl_2 at −95 °C and under red-light conditions, eq 1. The low temperature was needed to limit overoxidation to the SO_2-bridged complex BnS{Mo_2}-SO_2, **3**, although some of that product remained unavoidable. Separation required column chromatography. The synthesis of **1** has been completely revamped, still using *m*-$ClC_6H_4CO_3H$ but now in Me_2CO at 0 °C in the presence of excess acids. No special lighting conditions are needed. The new method is better for avoiding by-production of BnS{Mo_2}SO_2, **3**. Purification of the desired BnS{Mo_2}SO, **1**, product from unreacted BnS{Mo_2}S, **2**, and from small amounts of some other impurities can be done without chromatography. The purification takes advantage of the tenacious binding of BnS{Mo_2}SO, **1**, to silica gel from CH_2Cl_2 solution, while unreacted BnS{Mo_2}S and some impurities wash right through. The desired BnS{Mo_2}SO is then released from the silica gel with Me_2CO.

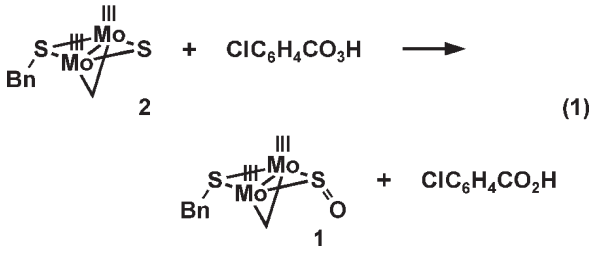

The peroxide reaction is conducted in the presence of excess HBF_4 and $MeCO_2H$, which keep the nascent product protonated,[34] thus inhibiting a second oxygenation. There is an additional reason for the excess $MeCO_2H$ and that is to avoid exchange of the carboxylate bridge from the dimolybdenum core; otherwise, *m*-chlorobenzoate exchanges for acetate to a slight extent. Neutralization of all acids afterward with aqueous $NaHCO_3$ gives dark-olive BnS{Mo_2}SO, **1**. Mechanistically, the peracid/acid/ketone combination could conceivably involve various peroxy intermediates,[35] leaving open the question of the actual oxidant. This possibility is noted but was not further investigated.

At the time of the original report,[17] BnS{Mo_2}SO, **1**, was believed to be photolytically and thermally unstable. Most issues regarding the instabilities have been eliminated or at least identified. The compound has good solution stability, giving 1−2% decomposition after six days in $CDCl_3$ (air-exposed) in the dark. The purified compound is only slightly light-sensitive: photolysis of a solution in $CDCl_3$ in an NMR tube in a 12-in., 32-W fluorescent ring lamp for 16 h yielded 1−2% reaction. This does not warrant reduced light conditions for normal handling. Crystalline **1** does undergo a very slow, clean reaction in the solid state, and the compound is best stored cold. In addition to these very slow processes, BnS{Mo_2}SO, **1**, does have one peculiar thermal habit: it decomposes relatively quickly while standing after evaporation from solution. This decomposition as a film is faster than as a crystalline solid and faster than when dissolved in solution. For this reason, postevaporation workup steps must be promptly executed until a crystallization step is reached. This postevaporation sensitivity was not recognized at the time of the original report. Further details of the crystal-phase and postevaporative reactions of BnS{Mo_2}SO are given below, following some related reactions.

Solution Reactions. BnS{Mo_2}SO, **1**, is considerably nucleophilic. Reaction of **1** with an alkyl halide, RX, in $(CD_3)_2CO$ gives *O*-alkylation, eq 2, resulting in the cationic complexes BnS{Mo_2}SOR^+, $\mathbf{4}^+$. Alkylation at O to give a thioperoxide linkage was definitive by isolation and characterization of the complexes $\mathbf{4}^+$ (vide infra). Alkylation at S to give a sulfinyl bridge (S(=O)R) was conceivable, but this outcome has never been identified in the present system of compounds.

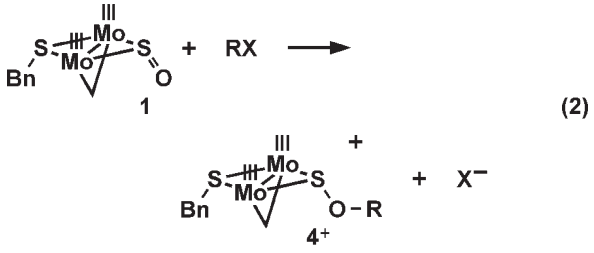

Studies of eq 2 are complicated by secondary reactions. The cations $\mathbf{4}^+$ are now electrophilic and are themselves vulnerable to attack by nucleophile, including attack by the halide anion coproduct. These secondary reactions parallel those from prior studies, which showed that bis (thiolate-bridged) cations of general formula R′S{Mo_2}-SR'^+ were subject to nucleophilic attack via two pathways, as illustrated by *a* and *b* below.[36]

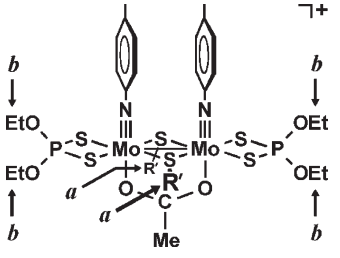

In path *a*, the nucleophile attacked either of the bridge thiolates at the α-carbon, cleaving the C−S bond to produce a neutral sulfide product R′S{Mo_2}S, **2**; this was a reversible equilibrium process. In path *b*, the nucleophile attacked either dithiophosphate ligand at either of its ethyl groups, cleaving a C−O bond; this was an irreversible de-esterification which gave neutral $[Mo_2(NTo)_2(S_2P(OEt)_2)(S_2PO(OEt))(\mu\text{-}O_2CMe)(\mu\text{-}SR')_2]$. This product contained one dianionic, monoethyl, dithiophosphate ligand, $(EtO)P(=O)S_2^{2-}$. Given the precedent of those studies, the analogous reactions for the current cations $\mathbf{4}^+$ are given by the debenzylation of eq 3 and the de-ethylation of eq 4.

(34) Protonation and hydrogen bonding studies remain in progress.

(35) Lange, A.; Brauer, H.-D. In *Peroxide Chemistry*; Waldemar, A., Ed.; Wiley-VCH Verlag: Weinheim, Germany, 2001; pp 157−176. Renz, M.; Meunier, B. *Eur. J. Org. Chem.* **1999**, 737–750. Murray, R. W. *Chem. Rev.* **1989**, *89*, 1187–1201.

(36) Koffi-Sokpa, E. I.; Calfee, D. T.; Allred, B. R. T.; Davis, J. L.; Haub, E. K.; Rich, A. K.; Porter, R. A.; Mashuta, M. S.; Richardson, J. F.; Noble, M. E. *Inorg. Chem.* **1999**, *38*, 802–813.

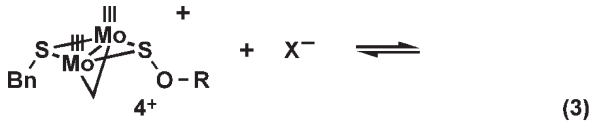

(3)

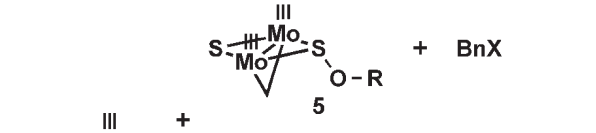

(4)

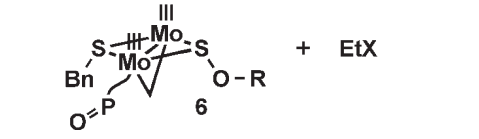

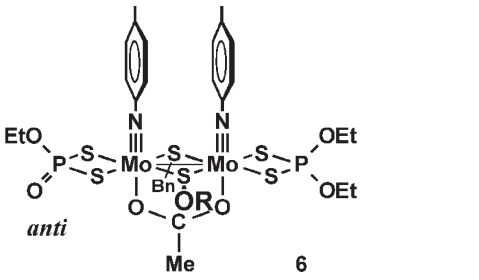

(The bracket notation, {Mo_2(P═O)}, and the stick diagram for **6** are modified to denote the presence of the modified dithiophosphate. For fuller illustration, a broadside view for this product is given above with eq 4.) Thus and overall, the reaction of starting sulfoxide BnS{Mo_2}SO, **1**, with alkyl halide proceeds first by *O*-alkylation, eq 2, to produce cation $\mathbf{4}^+$. Cation $\mathbf{4}^+$ can then undergo debenzylation (eq 3) to give S{Mo_2}-SOR, **5**, or cation $\mathbf{4}^+$ can undergo de-ethylation (eq 4) to produce BnS{Mo_2(P═O)}SOR, **6**.

As a specific example of the full sequence, the reaction of BnS{Mo_2}SO, **1**, with 1 equiv of benzyl bromide after 2 h in $(CD_3)_2CO$ showed 3% of the cation BnS{Mo_2}-$SOBn^+$, $\mathbf{4}^+$ (eq 2); 15% S{Mo_2}SOBn, **5** (eq 2 then eq 3); and 2% BnS{Mo_2(P═O)}SOBn, **6** (eq 2 then eq 4). A total of 79% BnS{Mo_2}SO, **1**, remained, and ~1% was not identified. The product distribution indicated that eq 3 was relatively fast and nascent $\mathbf{4}^+$ more promptly formed **5**. The reaction was also attempted using ethyl bromide, which gave no observable reaction after 2 h but yielded ~2% SMo_2SOEt, **5**, after 8 h.

Although the cationic complexes $\mathbf{4}^+$ are vulnerable to nucleophilic counterions, these could be separately prepared in pure form with triflate counterions. This allowed for a study of eqs 3 and 4 without starting from eq 2. For example, the reaction of BnS{Mo_2}$SOMe^+$ $CF_3SO_3^-$ ($\mathbf{4}^+CF_3SO_3^-$) in $(CD_3)_2CO$ with a limiting amount (0.5 equiv) of PPN^+ Cl^- gave, after 15 min, a product distribution of 69% S{Mo_2}SOMe, **5**, due to debenzylation (eq 3) and 31% BnS{Mo_2(P═O)}SOMe, **6**, due to de-esterification (eq 4). The reaction using BnS{Mo_2}$SOEt^+$ gave a similar product distribution. The byproducts BnCl (eq 3) and EtCl (eq 4) were seen in the ^{1}H NMR spectra. Notably, there was no evidence for BnS{Mo_2}SO, **1**, meaning attack at μ-SOR did not occur and eq 2 was not reversible.

In all of the solution-based de-esterification reactions of eq 4, two phosphoryl isomers are observed for the products BnS{Mo_2(P═O)}SOR, **6**. The isomers arise from attack at either of the two inequivalent ethyl arms on each dithiophosphate ligand. Using the tolylimido ligands as a directional reference, the isomers are denoted as anti or syn. The anti phosphoryl isomer was shown above with eq 4; the syn phosphoryl isomer is shown below. The isomers did not interconvert, and their relative formation was thus under kinetic control. Attack at the anti OEt position to give anti P═O is preferred. For example, the reaction of Cl^- with BnS{Mo_2}$SOMe^+$ $CF_3SO_3^-$ resulted in 77% of the anti phosphoryl isomer of BnS{Mo_2(P═O)}SOR, **6**.

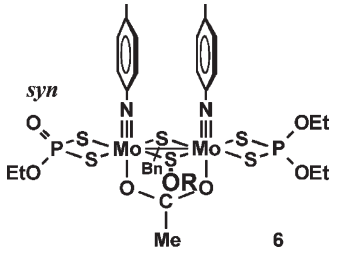

Interestingly, although eqs 3 and 4 complicated the studies of the nucleophilicity of the μ-SO bridge toward alkyl halides, these complications do extend the related chemistry of the system overall. Equation 3 provides a synthetic entry to the neutral compounds, S{Mo_2}SOR, **5**. Reactions similar to eqs 2 and 4 provide for a solid-state reaction of BnS{Mo_2}SO, **1**, itself, wherein the SO bridge is the nucleophile and a dithiophosphate ethyl group is the electrophile. This proved to be the manner of thermal decomposition of crystalline **1**.

Crystal-Phase Reaction of BnS{Mo_2}SO, 1. Crystalline batches of BnS{Mo_2}SO, **1**, undergo a slow decomposition in the solid state. Various trials were conducted to study the effects of different storage atmospheres, temperatures, and light levels. Of the variables, only temperature had an effect. As an example, a sample stored under a vacuum at normal room conditions decomposed 14% after 159 days, while an air-exposed sample in the freezer showed no reaction in the same time. On a shorter time scale, decomposition at room temperature was ~1% in 7 days. The reaction was very clean at room temperature, producing a single product, BnS{Mo_2(P═O)}SOEt, **6** (R = Et). Formally, this is tantamount to an isomerization: a dithiophosphate ethyl group ends up on the oxygen of the bridge SO moiety. The actual mechanism, however, is intermolecular, and it involves mutual attack between neighboring molecules within the crystal lattice.

The crystal structure of BnS{Mo_2}SO has been reported previously.[17] A re-examination of the packing has revealed that the molecules pair off in close approach for nucleophilic attack upon each other, as shown in Figure 1. The neighboring molecules are related by inversion. The oxygen atom of one molecule's SO bridge is 3.52(1) Å from the α-carbon of an ethyl group of a

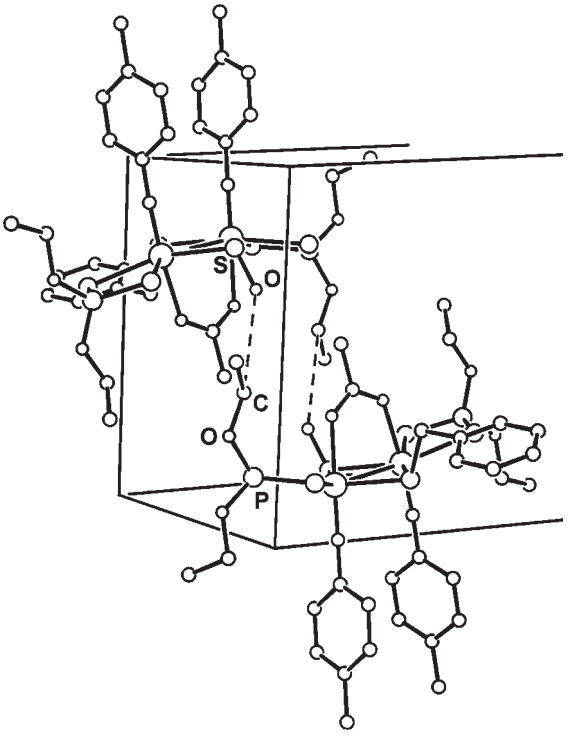

Figure 1. Nucleophilic faceoff between adjacent molecules in the crystal structure of BnS{Mo_2}SO, **1**. The dashed lines connect an oxygen from the SO bridge of one molecule to a dithiophosphate α-carbon on the adjacent molecule. Only one interaction is labeled, but the interactions are reciprocal.

dithiophosphate ligand on the adjacent molecule. This distance is close to but longer than a simple van der Waals contact (3.32 Å[37]). The angle of the approach, O···C−O, is 166(1)°, facilitating a backside attack. These interactions are reciprocal for each molecule in the pair. It is this fortuitous juxtaposition coupled with the inherent nucleophilicity of the bridge (S)O which provides for the solid-state reaction. While the attacks are mutual between the neighbors, they may or may not be mechanistically concerted.

As noted for the solution studies of eq 4, the ethyl arms of each dithiophosphate ligand are not equivalent, and de-esterification in solution gave both *anti*- and *syn*-BnS{Mo_2(P═O)}SOR, **6**. For the solid-state reaction of BnS{Mo_2}SO, **1**, however, only one isomer of **6** is obtained. The solid-phase juxtaposition of the bridge (S)O is to the anti ethyl arm of the dithiophosphate on the neighboring molecule. This orientation gives product **6** as the anti phosphoryl isomer only. This configuration was confirmed crystallographically for **6** as synthesized in this manner (vide infra).

Although the crystals for the previously reported crystal structure were obtained from CH_2Cl_2/MeOH, routine preparations have been more recently obtained from EtOH/H_2O or similar crystallization. Crystals obtained from EtOH/H_2O were examined for unit cell dimensions, and all of the *a*, *b*, *c*, and β values were within 0.2% of the values for the unit cell of the published crystal. The change in crystallization methods produced the same crystal morphology and is therefore believed to have left the crystal structure unchanged.

(37) Bondi, A. *J. Phys. Chem.* **1964**, *68*, 441–451.

While slow at room temperature, the solid reaction is faster at elevated temperatures. Synthetic procedures adopted a boiling water bath, and cooking the solid for 135−160 min gave complete reaction. Several impurities were also observed using the higher temperature, but these were in the 3−5% range total.

Postevaporation Decomposition of BnS{Mo_2}SO, 1. While the crystalline decomposition of BnS{Mo_2}SO, **1**, at room temperature proved to be slow, clean, and tidily resolved, the sensitivity of this compound to decomposition following evaporation from solution was more complicated. This evaporative decomposition was interesting in that it was much faster than the crystalline decomposition at room temperature and much faster than any decomposition in solution. For example, allowing a solution in EtOH to evaporate on a watch glass and then allowing the residue to stand open to the air for 3 h resulted in ∼4% decomposition (as determined by NMR after redissolving in $CDCl_3$). By comparison, an NMR-tube sample of **1** after 3 h in air-exposed 9:1 EtOH/D_2O showed no reaction at all. Thus, evaporation to a film predisposed **1** to decomposition. This was also peculiar to **1**: a similar evaporation trial using an EtOH solution of BnS{Mo_2}SOEt$^+$$CF_3SO_3^-$ (**4**$^+$$CF_3SO_3^-$) gave no reaction at all after a 3 h stand time, although such cations, **4**$^+$, are activated to nucleophilic attack.

Numerous studies of solutions of **1** were conducted involving various evaporation methods followed by a stand period of various times and conditions. Comparison was made for rotavapping, open-air evaporation, and stripping on a vacuum line, as well as for various solvents. Stand periods were conducted open to the air, open to the air in a jar at 100% relative humidity, open to dry N_2, open to dry O_2, and under vacuum conditions, and for various periods of time. Even the substrate of the evaporation vessel was studied, using standard (borosilicate) glass, polypropylene, or stainless steel. Samples were then redissolved in $CDCl_3$ and analyzed by NMR spectroscopy.

The decomposition occurred primarily during the stand time and not during the evaporation itself. The primary culprit causing decomposition was moisture, either atmospheric or water added to the solvent prior to evaporation. All substrates gave some decomposition, and glass gave the most. This was attributed to a simple film effect, since evaporation from polypropylene tended to give less of a film and more small crystals. Some decomposition was found in all of the solvents tested, including EtOH, Me_2CO, CH_2Cl_2, and MeCN.

The products of the decomposition clearly resulted from nucleophilic attack. For a more extensive run which involved evaporation from EtOH with a stand time of 22 h, 11% total decomposition was obtained. Some cations, **4**$^+$, were present, possibly BnS{Mo_2}SOEt$^+$ and BnS{Mo_2}SOBn$^+$, but these were not conclusively resolved. These cations represented the initial products of the attack of BnS{Mo_2}SO, **1**, on another molecule of **1** or, more likely, on its hydrate (possibly hydrogen-bonded[34]), thereby conceivably explaining the role of moisture. Identifications of S{Mo_2}SOEt, **5**, and of

$BnS\{Mo_2(P{=}O)\}SOEt$, **6** (major product), were definitive in the mixture; these arose from secondary processes. Other products were also present in small amounts. While fuller mechanistic details were not attempted, the general results did additionally demonstrate the nucleophilicity of **1**. Since the observed rates were not found in solution even with 10% D_2O (and given that crystalline **1** is prepared from aqueous media), then a film effect and moisture were jointly responsible. This presumably involved another proximity/orientation effect within the film.

Syntheses and Characterizations. The various reactions described herein are substantiated by isolation and characterization of representative compounds of types $\mathbf{4}^+$, **5**, and **6**.

The isolation of the cations $BnS\{Mo_2\}SOR^+$, $\mathbf{4}^+$, required the use of relatively non-nucleophilic counterions. Triflate salts were readily prepared from the reaction of $BnS\{Mo_2\}SO$, **1**, with methyl and ethyl triflates, as per eq 2 with RX = RO_3SCF_3. The products $\mathbf{4}^+CF_3SO_3^-$ were characterized by IR spectroscopy, NMR spectroscopy, and, in the case of $\mathbf{4}^+(Et)CF_3SO_3^-$, X-ray crystallography. The IR spectra showed the ancillary ligand sets and the triflate anion; no S−O vibrations from the bridge SOR group could be definitively distinguished from the other absorptions present in the range of interest. (Reported values for ν(SO) range from 650 to 760 cm^{-1} for various RSOR and related derivatives.[32,38−40] The range extends to ∼800 cm^{-1} with strong electron withdrawal.[41,42]) ^{31}P and ^1H NMR spectra gave all of the appropriate resonances. The ^1H chemical shifts of the α-hydrogens of the thioperoxide R groups were relatively downfield, consistent with alkylation at O and not at S. X-ray crystallography for $\mathbf{4}^+(Et)CF_3SO_3^-$ definitively confirmed the S−O−Et linkage arising from *O*-ethylation as opposed to a sulfinyl ligand, S(=O)Et, arising from *S*-ethylation.

The NMR spectra also revealed conformational isomers in solution associated with facile inversion at the pyramidal sulfur bridges; these invertomers are common to $BnS\{Mo_2\}SO$, **1**,[17] to previously reported $R'S\{Mo_2\}SR'^+$ cations,[36] and to other prior compounds. The sulfur substituent positions are labeled distal (*d*) or proximal (*p*) relative to the tolylimido rings as a reference point. Cations $\mathbf{4}^+$ have four possible isomers, shown below as isomers A−D. The isomer distribution in $CDCl_3$ for $\mathbf{4}^+$(Me) is 76% A, 16% B, and 9% C; the distribution for $\mathbf{4}^+$(Et) is the same within integration error. The presence of isomer D was not definitive for either compound in $CDCl_3$, but this was present at ∼1% in $(CD_3)_2CO$.

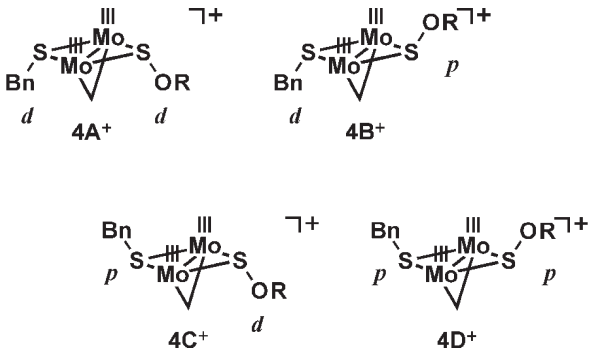

Turning now to neutral $S\{Mo_2\}SOR$, **5** (R = Me, Et), these were prepared from the debenzylation of the cations $BnS\{Mo_2\}SOR^+$, $\mathbf{4}^+$, per eq 3. Competition from eq 4 could not be eliminated, and this necessitated some optimization work. First, the choice of benzyl thiolate as one bridge in the reactant $BnS\{Mo_2\}SOR^+$, $\mathbf{4}^+$, was ultimately to allow for facile C−S cleavage; methyl thiolate or ethyl thiolate bridges could not dealkylate quickly enough to compete with eq 4. Second, various nucleophiles were also examined for enhancing the selectivity of $S\{Mo_2\}SOR$, **5**, over the de-esterification product **6**. Tested nucleophiles included Cl^-, Br^-, and I^- (as PPN^+ salts); Ph_3P; and Et_3N. PPN^+I^- proved the most useful reagent for synthetic purposes.

While the methyl and ethyl derivatives $S\{Mo_2\}SOMe$ and $S\{Mo_2\}SOEt$ were synthesized from cations $\mathbf{4}^+$, it proved possible to synthesize the benzyl derivative $S\{Mo_2\}SOBn$ directly from $BnS\{Mo_2\}SO$, **1**, by reaction with excess benzyl bromide. The one-pot synthesis combined eq 2 and eq 3, while trying to avoid eq 4. The ability to isolate product **5** cleanly by this route was only successful for R = Bn due to the facile kinetics of benzyl displacement. Interestingly, this reaction is also tantamount to isomerization, but the process is again intermolecular.

The products $S\{Mo_2\}SOR$, **5** (R = Me, Et, Bn), were characterized by IR spectroscopy and NMR spectroscopy, along with X-ray crystallography for $S\{Mo_2\}SOEt$. The IR spectra again showed the usual ligand sets but no definitive S−O vibration. The NMR spectra showed all of the appropriate resonances. The chemical shifts of the R groups were relatively downfield again, indicating that the thioperoxide linkage was preserved as S−O−R. X-ray crystallography for $S\{Mo_2\}SOEt$ confirmed the structure. These compounds are isostructural to the disulfides $S\{Mo_2\}SSR$, which have been previously characterized, including the R = Et and Bn derivatives.[43]

The NMR spectra of $S\{Mo_2\}SOR$, **5**, again revealed sulfur invertomers, but now only two isomers were possible, depending on whether the thioperoxide group was distal or proximal. The invertomer ratios (distal/proximal) in $CDCl_3$ were 18 for $S\{Mo_2\}SOMe$, 3.8 for $S\{Mo_2\}SOEt$, and 3.9 for $S\{Mo_2\}SOBn$. The latter two ratios are similar to the invertomer ratios of 4 and 6 for the disulfides $S\{Mo_2\}SSEt$ and $S\{Mo_2\}SSBn$, respectively.

The de-esterification product $BnS\{Mo_2(P{=}O)\}SOEt$, **6**, was synthesized from the thermal decomposition of

(38) Steudel, R.; Schmidt, H.; Baumeister, E.; Oberhammer, H.; Koritsanszky, T. *J. Phys. Chem.* **1995**, *99*, 8987–8993.
(39) Reina, M. C.; Boese, R.; Ge, M.; Ulic, S. E.; Beckers, H.; Willner, H.; Della Védova, C. O. *J. Phys. Chem. A* **2008**, *112*, 7939–7946.
(40) Brown, C.; Hogg, D. R.; McKean, D. C. *Spectrochim. Acta* **1970**, *26A*, 39–42.
(41) Ulic, S. E.; von Ahsen, S.; Willner, H. *Inorg. Chem.* **2004**, *43* 5268–5274.
(42) Ulic, S. E.; Della Védova, C. O.; Hermann, A.; Mack, H.-G.; Oberhammer, H. *Inorg. Chem.* **2002**, *41*, 5699–5705.
(43) Noble, M. E. *Inorg. Chem.* **1986**, *25*, 3311–3317.

crystalline BnS{Mo_2}SO, **1**. The IR spectrum again showed the usual ligand set and again gave no clearly assignable SO band, but now there was a clear phosphoryl stretch at 1219 cm^{-1}. The NMR spectra were more complex due to the reduced symmetry within the molecule, which was now asymmetric. In addition, sulfur invertomers were again observed due to pyramidal fluxionality. Of the four possible sulfur invertomers, only two were seen in $CDCl_3$, and these paralleled isomers A and B, as illustrated above for the cations $\mathbf{4}^+$. Only the anti phosphoryl isomer was produced in the solid-state reaction, and thus, only one phosphoryl isomer is noted here.

For the dominant sulfur invertomer, the ^{31}P NMR spectrum showed the $(EtO)_2PS_2^-$ ligand at 111.8 ppm and the $(EtO)(O)PS_2^{2-}$ ligand at 76.3 ppm. The downfield peak showed a PP coupling of 1.5 Hz, but this was not resolved in the upfield peak due to its greater broadness (7 Hz linewidth). In the ^1H NMR spectrum, the loss of symmetry was particularly apparent in the geminal coupling of inequivalent CH_2 protons within each of the SBn and the SOEt bridge groups.

In addition to the spectroscopic evidence, X-ray crystallography again confirmed the structure.

Within the various compounds $\mathbf{4}^+$, **5**, and **6**, preliminary studies of the reactivity of the thioperoxide unit have demonstrated a reasonable stability. The compounds have an excellent shelf life. For example, after typical benchtop, room-temperature, air-exposed storage, solid samples of BnS{Mo_2}SOEt$^+$ ($\mathbf{4}^+$) $CF_3SO_3^-$ and of S{Mo_2}SOMe (**5**) were unchanged after one year. BnS{Mo_2}SOEt$^+CF_3SO_3^-$ is also stable after five days in air-exposed, $CDCl_3$ solution. Attempts to isomerize the thioperoxide to a sulfinyl ligand using thermal or photolytic methods have so far been unsuccessful or, at least, inconclusive. Unfortunately, at the high temperatures and or UV irradiation required to get any kind of reaction, the acetate and dithiophosphate coligands also become reactive, thus rendering these efforts difficult. Attempts to observe S−O bond homolysis have likewise been inconclusive, despite the straightforward photohomolysis previously reported for the disulfides S{Mo_2}SSR.[44]

Crystallographic Studies. Four crystal structures are presented which contain the *O*-ethyl thioperoxide ligand, $EtOS^-$, bridging in μ_2-η^1(*S*) fashion. ORTEP views[45] are shown in Figures 2−5, and selected metrical results are in Tables 1 and 2. Full tabulations are provided in the Supporting Information. Cations $\mathbf{4}^+$ are represented by BnS{Mo_2}SOEt$^+$; this structure is compared to that of the precursor BnS{Mo_2}SO, **1**, for the effects of alkylation at O. Compounds **5** are represented by two structures of S{Mo_2}SOEt, for which crystals of both sulfur invertomers were fortuitously obtained. The structure of this thioperoxide compound is also compared to that of the disulfide analog, S{Mo_2}SSEt.[46] Compounds **6** are represented by BnS{Mo_2(P═O)}SOEt; in addition to the thioperoxide ligand, this compound also provides another structural characterization of a dianionic, monoalkyl dithiophosphate ligand. The additional interest

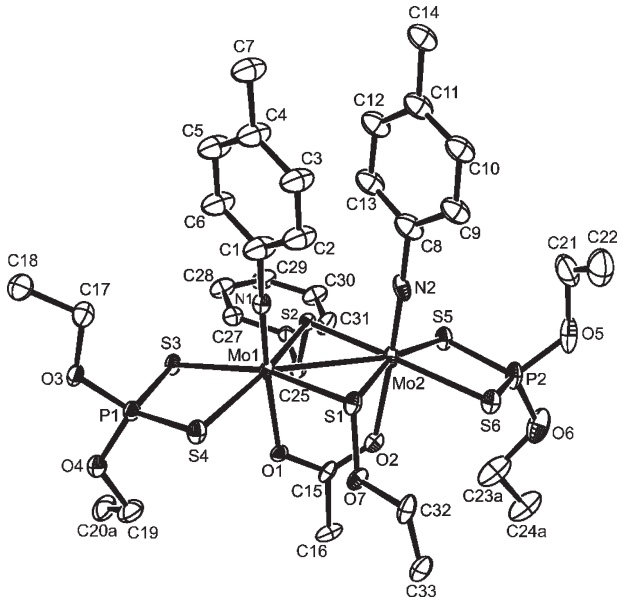

Figure 2. ORTEP view of the cation BnS{Mo_2}SOEt$^+$, $\mathbf{4}^+$(Et).

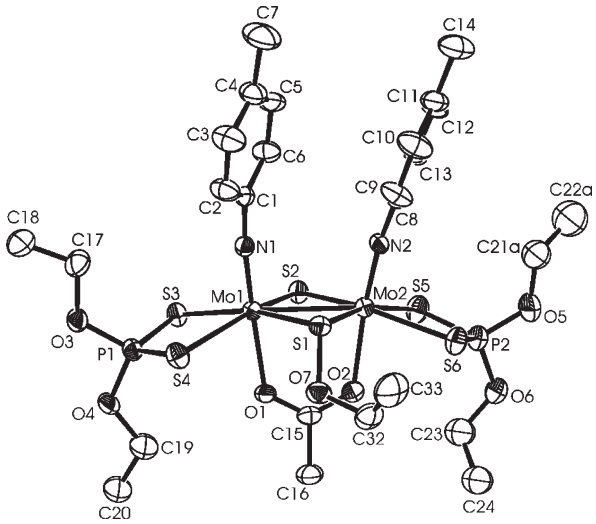

Figure 3. ORTEP view of the distal isomer of S{Mo_2}SOEt, **5**(Et).

therein lies in the fact that there are few structural studies known for this ligand,[47−49] in stark contrast to the extensive characterization of monoanionic, dialkyl dithiophosphate ligands.

Most of the general features of the underlying Mo_2−dithiophosphate−acetate−tolylimido frameworks are similar to those of prior compounds and will not be considered here. The emphasis here is the thioperoxide ligand itself and its effects, if any, on the dimolybdenum cores. The one exception will include additional description of the monoethyl $(EtO)(O)PS_2^{2-}$ ligand in **6** since a prior structure of this ligand type had some disorder. Throughout, any comparisons of metric data here to data of prior structures will be done following the numbering scheme as used in the present report, regardless of the atom-numbering system used in the previous reports.

(44) Lizano, A. C.; Munchhof, M. G.; Haub, E. K.; Noble, M. E. *J. Am. Chem. Soc.* **1991**, *113*, 9204–9210.
(45) Farrugia, L. J. *J. Appl. Crystallogr.* **1997**, *30*, 565.
(46) Noble, M. E.; Williams, D. E. *Inorg. Chem.* **1988**, *27*, 749–752.
(47) Boíllos, E.; Miguel, D. *Organometallics* **2004**, *23*, 2568–2572.
(48) Abram, U.; Ritter, S. *Inorg. Chim. Acta* **1993**, *210*, 99–105.
(49) Gastaldi, L.; Porta, P.; Tomlinson, A. G. *J. Chem. Soc., Dalton Trans.* **1974**, 1424–1429.

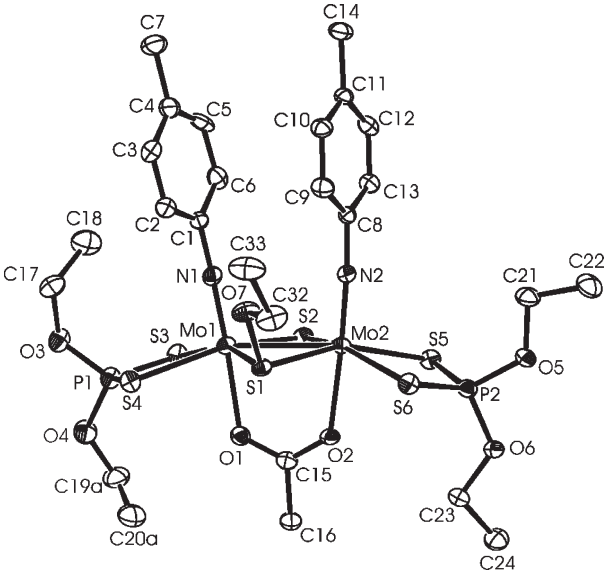

Figure 4. ORTEP view of the proximal isomer of S{Mo_2}SOEt, **5**(Et).

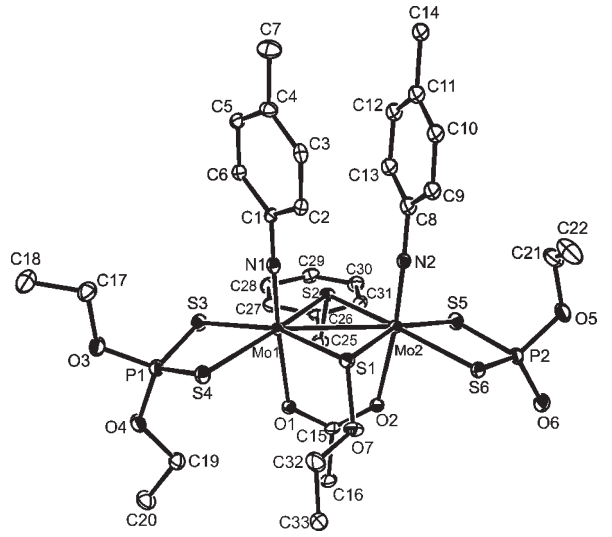

Figure 5. ORTEP view of BnS{Mo_2(P═O)}SOEt, **6**(Et).

A comparison of the thioperoxide ligand itself among the four structures shows the S(1)−O(7) bond lengths to be identical in the three distal isomers (1.655(5) Å, 1.654(3) Å and 1.655(3) Å), while that in the one proximal isomer (1.666(4) Å) was similar within error. The O(7)−C(32) bond lengths range from 1.429(6) to 1.466(8) Å. The angle at O(7) shows a little flex, 112.0(3)−116.7(3)°. The sulfur is distinctly pyramidal in all four cases, with the sum of angles at S(1) ranging 287.3(2) to 293.1(2)°. Aside from this last parameter, the other values are comparable to metric results reported for several known RSOR structures and related derivatives.[38,39,50−52]

Table 1. Selected Bond Lengths (Å)

	4$^+$	**5**, distal	**5**, proximal	**6**
Mo(1)−Mo(2)	2.8807(9)	2.8518(7)	2.8419(7)	2.9109(7)
Mo(1)−S(1)	2.4378(17)	2.4401(14)	2.4176(13)	2.4566(9)
Mo(1)−S(2)	2.4454(18)	2.3457(14)	2.3543(14)	2.4416(10)
Mo(2)−S(1)	2.4436(19)	2.4565(14)	2.4370(13)	2.4433(10)
Mo(2)−S(2)	2.4382(17)	2.3439(14)	2.3564(13)	2.4542(10)
Mo(1)−S(3)	2.4917(17)	2.5176(14)	2.5175(14)	2.5092(10)
Mo(1)−S(4)	2.5144(19)	2.5695(14)	2.5580(14)	2.5386(10)
Mo(2)−S(5)	2.4969(19)	2.5173(16)	2.5208(14)	2.4725(10)
Mo(2)−S(6)	2.495(2)	2.5726(15)	2.5547(13)	2.4616(10)
Mo(1)−N(1)	1.721(6)	1.731(4)	1.732(4)	1.735(3)
Mo(2)−N(2)	1.718(6)	1.737(4)	1.734(4)	1.734(3)
Mo(1)−O(1)	2.156(4)	2.169(3)	2.196(3)	2.135(2)
Mo(2)−O(2)	2.169(5)	2.168(3)	2.199(3)	2.171(2)
S(1)−O(7)	1.655(5)	1.654(3)	1.666(4)	1.655(3)
O(7)−C(32)	1.466(8)	1.429(6)	1.438(6)	1.456(5)
C(32)−C(33)	1.513(12)	1.468(8)	1.499(8)	1.502(6)
P(1)−S(3)	2.011(3)	1.9983(19)	1.994(2)	2.0068(14)
P(1)−S(4)	1.998(2)	1.990(2)	1.9923(19)	1.9912(13)
P(1)−O(3)	1.579(5)	1.574(3)	1.585(4)	1.566(3)
P(1)−O(4)	1.553(5)	1.567(3)	1.573(4)	1.572(3)
O(3)−C(17)	1.431(9)	1.479(6)	1.451(7)	1.461(5)
O(4)−C(19)	1.485(10)	1.459(7)	dis[a]	1.463(4)
P(2)−S(5)	1.998(3)	1.994(2)	2.0003(19)	2.0560(14)
P(2)−S(6)	2.014(3)	1.988(2)	1.9897(19)	2.0550(14)
P(2)−O(5)	1.567(7)	1.577(4)	1.575(4)	1.595(3)
P(2)−O(6)	1.563(7)	1.574(4)	1.569(4)	1.470(3)
O(5)−C(21)	1.570(14)	dis[a]	1.459(6)	1.451(5)
O(6)−C(23)	dis[a]	1.443(7)	1.465(6)	

[a] Values involving a disorder are not listed here but may be found in the Supporting Information.

Table 2. Selected Bond and Dihedral Angles (deg)

	4$^+$	**5**, distal	**5**, proximal	**6**
S(1)−Mo(1)−S(2)	107.60(6)	107.15(5)	106.96(5)	107.04(3)
S(1)−Mo(2)−S(2)	107.65(6)	106.67(5)	106.26(5)	107.07(3)
S(3)−Mo(1)−S(4)	79.50(6)	77.95(5)	78.10(5)	78.28(3)
S(5)−Mo(2)−S(6)	79.47(7)	77.32(5)	78.15(4)	79.46(3)
O(1)−Mo(1)−N(1)	175.1(2)	169.11(15)	170.05(17)	174.20(11)
O(2)−Mo(2)−N(2)	177.5(2)	165.47(15)	172.72(17)	174.55(11)
Mo(1)−S(1)−Mo(2)	72.33(5)	71.24(4)	71.66(4)	72.89(3)
Mo(1)−S(1)−O(7)	106.87(18)	108.19(13)	108.54(14)	110.07(10)
Mo(2)−S(1)−O(7)	108.18(19)	113.69(13)	111.85(15)	104.30(10)
sum of angles at S(1)	287.4(3)	293.1(2)	292.0(2)	287.3(2)
Mo(1)−S(2)−Mo(2)	72.30(5)	74.91(4)	74.21(4)	72.96(3)
Mo(1)−S(2)−C(25)	110.1(2)			108.86(12)
Mo(2)−S(2)−C(25)	109.3(2)			110.21(12)
S(1)−O(7)−C(32)	113.7(5)	116.7(3)	112.0(3)	114.6(2)
S(3)−P(1)−S(4)	105.99(11)	106.72(8)	106.68(8)	105.68(6)
S(5)−P(2)−S(6)	105.40(12)	105.99(9)	106.62(8)	100.19(5)
O(3)−P(1)−O(4)	98.0(3)	97.12(19)	96.8(2)	95.31(14)
O(5)−P(2)−O(6)	98.2(4)	96.6(2)	95.77(19)	106.39(15)
Mo(1)−S(1)−O(7)-C(32)	175.8(4)	156.7(3)	174.0(4)	89.0(3)
Mo(2)−S(1)−O(7)-C(32)	107.8(4)	79.7(4)	96.9(4)	165.7(2)
S(1)−Mo(1)−Mo(2)-S(2)	176.85(8)	178.38(6)	171.24(6)	178.44(4)

For those, S−O bond lengths ran 1.625(2)−1.663(5) Å, O−C(alkyl) bond lengths ran 1.426(3)−1.45(2) Å, and angles at O ran 113(2)−117(2)°. As a further comparison of note, there is even some manifestation of the dihedral preference within the thioperoxide ligand in the present compounds. Dihedral angles about S−S, S−O, and O−O bonds have been of considerable interest for many years, and especially recently for RSOR derivatives.[50,51,53]

(50) Ulic, S. E.; Kosma, A.; Della Védova, C. O.; Willner, H.; Oberhammer, H. *J. Phys. Chem. A* **2006**, *110*, 10201–10205. Ulic, S. E.; Kosma, A.; Leibold, C.; Della Védova, C. O.; Willner, H.; Oberhammer, H. *J. Phys. Chem. A* **2005**, *109*, 3739–3744.

(51) Buschmann, J.; Luger, P.; Koritsanszky, T.; Schmidt, H.; Steudel, R. *J. Phys. Chem.* **1992**, *96*, 9243–9250.

(52) Cannon, D.; Low, J. N.; McWilliam, S. A.; Skakle, J. M. S.; Wardell, J. L.; Glidewell, C. *Acta Crystallogr., Sect. C* **2001**, *57*, 600–603. LaPlaca, S. J.; Ibers, J. A.; Hamilton, W. C. *J. Am. Chem. Soc.* **1964**, *86*, 2289–2290.

(53) Du, L.; Yao, L.; Ge, M. *J. Phys. Chem. A* **2007**, *111*, 11787–11792. Du, L.; Yao, L.; Zeng, X.; Ge, M.; Wang, D *J. Phys. Chem. A* **2007**, *111*, 4944–4949.

Experimental and calculated conformations prefer dihedral angles loosely near 90° (±20°), although some show an additional shallow minimum or flat potential near 180°. Interestingly, the S−O dihedral angles herein are within or close to those ranges even though the sulfur is now three-bonded, giving two dihedral values in each derivative, Mo(1)S−OC and Mo(2)S−OC. Overall, the thioperoxide ligand structurally parallels organic sulfenate derivatives, even in a bridging arrangement.

Turning now to the individual compounds, the general structure of the cation in $BnS\{Mo_2\}SOEt^+CF_3SO_3^-$ is the same as its major solution invertomer, with both bridge sulfur groups in distal orientation. Comparison of the crystal structure to that of the precursor $BnS\{Mo_2\}$-SO, **1**, reveals several effects of the alkylation at O. As expected, S(1)−O(7) lengthens considerably, from 1.515 (4) Å in **1** to 1.655(5) Å in $\mathbf{4}^+$. Both of the Mo−S(1)−O(7) angles decrease upon alkylation (113.1(2)° and 113.7(2)° in **1** vs 106.87(18)° and 108.18(19)° in $\mathbf{4}^+$), consistent with reduced steric demand upon changing from S=O to S−O. There is a corresponding effect on the pyramidicity of the sulfur: the sum of the angles at S(1) decreases from 299.2(3)° in **1** to 287.4(3)° in $\mathbf{4}^+$. This effect is specific to the thioperoxide S(1) bridge: by comparison, the sum of the angles at the benzyl thiolate sulfur, S(2), are more similar for the two compounds, 293.9(3)° in **1** versus 291.7 (3)° in $\mathbf{4}^+$. Mo−S(1) bond lengths are also close between the two compounds, 2.429(1) Å and 2.428(1) Å in **1** versus 2.4378(17) Å and 2.4436(19) Å in $\mathbf{4}^+$. The Mo−S(dithiophosphate) bonds which are trans to S(1) (namely, Mo-(1)−S(3) and Mo(2)−S(5)) contract a bit, 2.523(2) Å for each in **1** versus 2.4917(17) Å and 2.4969(19) Å in $\mathbf{4}^+$; this suggests a weakened trans influence upon alkylation at O.

Beyond these comparisons, there are other modest differences between $BnS\{Mo_2\}SOEt^+$ and $BnS\{Mo_2\}$-SO, but these differences are similar when comparing another cation, $MeS\{Mo_2\}SMe^+$,[36] to $BnS\{Mo_2\}SO$. Thus, those additional differences are not a consequence of the thioperoxide link.

Two crystal structures of $S\{Mo_2\}SOEt$, **5**, were obtained, differing in the invertomer orientation of the thioperoxide bridge. Chronologically, the proximal isomer was first, although this was not the dominant solution isomer. By varying solvent combinations, a crystal and a structure of the distal isomer were also obtained. The principal structural differences between the two isomers are parallel to the differences previously reported for the closely related (but not isomeric) dimolybdenum sulfenimines, $S\{Mo_2\}SN{=}CHCMe_3$ (distal) and $S\{Mo_2\}SN{=}CMe_2$ (proximal).[54] Thus, these differences are not associated with the thioperoxide ligand per se. The major reason for the specific interest in the distal isomer was in its isostructural relationship to the distal structure of the disulfide complex, $S\{Mo_2\}SSEt$,[46] thereby allowing a direct comparison of the ethyl thioperoxide $EtOS^-$ bridge to the ethyl persulfide $EtSS^-$ bridge. The $\{Mo_2\}$ frameworks are relatively unchanged: Mo−S(1) bond lengths are similar (2.4401(14) and 2.4565(14) in **5** vs 2.446(1) and 2.451(1) Å), as are trans Mo−S(dithiophosphate) bonds (2.5176(14) and 2.5173(16) vs 2.511(2) and 2.520(1) Å). Thus, these two functional groups impart no difference on the dimolybdenum framework. The bridge groups do show expected differences internally, with S−O at 1.654(3) Å versus S−S at 2.068(2) Å and O−C at 1.429(6) Å versus S−C at 1.789(7) Å. Chalcogen angles for the bridges are 116.7(3)° for ∠S−O−C versus 101.5(3)° for ∠S−S−C.

The crystal structure of the de-esterified product $BzS\{Mo_2(P{=}O)\}SOEt$, **6**, is the same as its major solution invertomer, again with both sulfur bridge substituents in distal orientation. An important feature of this structure lies in the definitive confirmation of conformation regarding the phosphoryl bond; this is in the anti position, reflecting the mode of attack in the crystal phase reaction of the precursor $BnS\{Mo_2\}SO$, **1**. A second importance lies in the $(EtO)OPS_2^{2-}$ ligand itself. The thioperoxide bridge in neutral **6** shows no significant changes relative to that in cation $\mathbf{4}^+$. The primary changes in comparing the overall structures of **6** and $\mathbf{4}^+$ arise from converting one monoanionic $(EtO)_2PS_2^-$ to a dianionic $(EtO)(O)PS_2^{2-}$, and these changes parallel a prior comparison for $EtS\{Mo_2(P{=}O)\}SEt$[36] which were not related to a thioperoxide bridge. A key feature of that compound as well as **6** is that they both contain a typical, monoanionic, diethyl dithiophosphate along with a dianionic, monoethyl dithiophosphate in otherwise equivalent environments; this allows a direct comparison of the two ligand types. Such a comparison for the prior compound, $EtS\{Mo_2(P{=}O)\}SEt$, was limited due to some disorder in the phosphoester functionality, but this is not the case for the present $BzS\{Mo_2(P{=}O)\}SOEt$, **6**.

The $(EtO)(O)PS_2^{2-}$ ligand of **6** possesses longer P(2)−S bonds (2.0560(14) and 2.0550(14) A) than the P(1)−S bonds in the $(EtO)_2PS_2^-$ ligand (2.0068(14) and 1.9912(13) A); this is consistent with formal bond orders of 1 versus 1.5. On the other hand, the dianion is a better donor than the monoanion, which gives shorter Mo−S (dithiophosphate) bonds: 2.4725(10) and 2.4616(10) Å for Mo(2)−S(5,6) versus 2.5092(10) and 2.5386(10) A for Mo(1)−S(3,4). Within the $(EtO)(O)PS_2^{2-}$ ligand itself, the phosphoryl P(2)=O(6) bond is much shorter, 1.470(3) Å, compared to the ester P(2)−O(5) bond of 1.595(3) Å; the latter is long compared to P(1)−O(3,4) lengths of 1.566(3) and 1.572(3) Å in the diester $(EtO)_2PS_2^-$. (P)O−C bond lengths are the same within error between the two dithiophosphate ligands, 1.451(5)−1.463(4) Å. The phosphoryl linkage opens the OPO angle to 106.39 (15)° for P(2) from 95.31(14)° for P(1); the SPS angle respectively closes to 100.19(5)° from 105.68(6)°. These results extend the resonance discussion, as had been presented for $EtS\{Mo_2(P{=}O)\}SEt$.[36]

Discussion

The complex $BnS\{Mo_2\}SO$, **1**, is somewhat of a paradoxical mix of nucleophilic character combined with weak electrophilic character. The SO bridge is considerably nucleophilic at O, reacting with classical electrophiles such as alkyl halides but also slowly on another molecule of its own type in its own crystal phase. In solution, alkylation at O gives an activated cation with enhanced electrophilicity at the benzyl thiolate and dithiophosphate ester sites.

(54) Haub, E. K.; Richardson, J. F.; Noble, M. E. *Inorg. Chem.* **1992**, *31*, 4926−4932.

While organic sulfoxides are nucleophilic at both S and O, no evidence has been seen in BnS{Mo_2}SO, **1**, for alkylation at S to produce a sulfinyl product, BnS{Mo_2}S(=O)R^+, although sulfinyl-bridged dimetal systems are indeed known.[55−57] This relative lack of reactivity at S may be kinetic or thermodynamic. Kinetic factors arise from the overhanging ortho positions of the imido rings, which provide some steric interference at the bridge sulfur positions. Although reaction at S is not seen in this work, the oxygenation of BnS{Mo_2}SO, **1**, to BnS{Mo_2}SO_2, **3**, had shown in prior work that the SO sulfur atom was not completely inert and that some reactivity at that site did still exist.[17] In contrast, the sulfur of the thiolate bridge has not shown any nucleophilicity in any work to date, and in fact, this sulfur tends to be dealkylated in some of these derivatives.

There is some precedent for *O*-alkylation at metal-SO sites among various $M_xS_yO_z$ systems. *O*-alkylation of a tri-iron SO_2 bridge was accomplished using MeO_3SCF_3;[58] a similar reaction with AcCl was proposed to give *O*-acetylation.[16] *O*-alkylation of an Ir−S_2O ligand was reported using MeO_3SF.[28] *O*-alkylations of sulfinyl or sulfonyl ligands are also known (or proposed), using alkyl halides or Et_3O^+ derivatives.[32,59,60] In addition to alkylation at O, sulfinyl metal systems, MS(=O)R, can also alkylate at S.[61]

Given the fundamental interest in the nucleophilicity of the SO functional group and its importance in the chemistry of organic sulfoxides, there is broad potential among either metallo forms, M_2(SO) or MS(=O)R, considering the possible variations in the metal, the d-electron count, coligands, M−S π bonding/antibonding character, and other factors, along with the interplay of such factors toward enhancing the classical polarized bond form ($\delta+$)S−O($\delta-$) of the sulfoxide linkage.[9,62] Difficulties in synthetic methodologies, however, impede such studies. Unfortunately, one of the best known reactions for these systems is further oxygenation to $M_2(SO_2)$ or MS(=O)$_2$R (or other products); such reactions are often facile and difficult to avoid synthetically. The protonation/deprotonation method reported herein proved very effective in protecting BnS{Mo_2}SO, **1**, from the second oxygenation.

As a ligand, the $^-$SOR thioperoxide bridge has proven to be fairly robust in the present systems so far, even outlasting some coligands under somewhat energetic conditions. The failure to achieve isomerization to a sulfinyl ligand may be an experimental difficulty or it may represent a thermodynamic preference, an outcome which is known for some sulfenate ester-sulfoxide conversions.[23,24,41,63]

Given the thioperoxide/sulfenate ester RSOR connection, the present compounds S{Mo_2}SOR, **5**, can be considered dimolybdenum sulfenate ester analogs. This consideration (moreso for **5** than for **4**$^+$ or **6** given the background of prior work) follows previous analogies of dimolybdenum sulfenyl types such as the primary sulfenamide S{Mo_2}SNH_2,[54,64] sulfenimines S{Mo_2}SN=CZ_2,[54] sulfenyl halides S{M_2}SX (more stable for M = W than for M = Mo),[65] and disulfides S{Mo_2}SSR.[43,46] Despite the fact that the sulfur is three-bonded in these complexes, other structural, spectroscopic, and chemical properties parallel such properties in $RSNH_2$, RSN=CZ_2, RSX, and RSSR.

The sulfenate character of the current system contrasts sharply with various sulfinyl ligand complexes which are termed sulfenates. There is reasonable cause for more uniform terminology for the various sulfur oxygenates within the inorganic and organic domains which span the general chemistry of sulfur.

Experimental Section

Reactions and manipulations were conducted open to the air, except as noted. BnS{Mo_2}S, **2**, was prepared as previously reported[43] or by an analogous procedure using BnCl in benzene instead of BnBr in CH_2Cl_2. *m*-Chloroperbenzoic acid was prepared for use by drying a small portion (<1 g) of the commercial impure reagent (containing water and *m*-chlorobenzoic acid) in a desiccator for several days. The peracid/acid content for each portion was then assessed from the ^{1}H NMR spectrum, and this was converted to mass percent. PPN^+I^- was prepared from PPN^+Cl^-.[66] Where indicated, "dry" CH_2Cl_2 was simply syringed from a settled slurry of solvent, $CaCl_2$, and $NaHCO_3$. Other solvents and reagents were used as received. Silica gel was Davisil grade 644. Except where indicated, operations were conducted open to the air. $^{31}P\{^1H\}$ and ^{1}H NMR spectra were obtained on a Varian Inova500 spectrometer; results are reported relative to external 85% H_3PO_4 and internal Me_4Si, respectively. Solution reactions were monitored by NMR spectroscopy in $(CD_3)_2CO$, except as noted. NMR characterization data were obtained in $CDCl_3$ and are reported below; values for the minor sulfur invertomers are given in parentheses when these were confidently discernible. When three or more isomers could be assigned, these were given by A for the major isomer, followed by B−D parenthetically for the other isomers. The A−D labels follow those diagrammed in the Results for **4**$^+$. Infrared spectra were obtained on a Mattson Galaxy Series FTIR 5000 spectrometer by diffuse reflectance on KBr powder.

BnS{Mo_2}SO, 1. This preparation is greatly improved over the prior method,[17] and no light exclusion is necessary. A solution of BnS{Mo_2}S, **2** (0.3701 g, 0.375 mmol) in 7.0 mL Me_2CO was chilled in an ice water bath. Separately, a solution of *m*-chloroperbenzoic acid (0.0719 g, 88%, 0.37 mmol) in 1.8 mL of Me_2CO was likewise chilled. To the stirring, red−orange solution of **2** were added in close succession $MeCO_2H$ (86 μL), HBF_4 (48% aqueous, 98 μL), and then, dropwise, the cold solution of *m*-chloroperbenzoic acid. Two rinses (0.5 mL each) with Me_2CO were used to facilitate the quantitative transfer of the peracid solution. The solution color changed to orange−yellow during the addition.

After stirring cold for 3 min, a solution (unchilled) of $NaHCO_3$ (0.2518 g, 3.00 mmol) in 4.0 mL of H_2O was slowly added,

(55) Vasyutinskaya, E. A.; Eremenko, I. L.; Pasynskii, A. A.; Nefedov, S. E.; Yanovskii, A. I.; Struchkov, Y. T. *Russ. J. Inorg. Chem.* **1991**, *36*, 964–972.
(56) Kramer, A.; Lingnau, R.; Lorenz, I.-P.; Mayer, H. A. *Chem. Ber.* **1990**, *123*, 1821–1826. Messelhäuser, J.; Gutensohn, K. U.; Lorenz, I.-P.; Hiller, W. *J. Organomet. Chem.* **1987**, *321*, 377–388.
(57) Silverthorn, W. E. *J. Organomet. Chem.* **1980**, *184*, C25–C27.
(58) Karet, G. B.; Norton, D. M.; Stern, C. L.; Shriver, D. F. *Inorg. Chem.* **1994**, *33*, 5750–5753.
(59) Schenk, W. A.; Bezler, J.; Burzlaff, N.; Hagel, M.; Steinmetz, B. *Eur. J. Inorg. Chem.* **2000**, 287–297.
(60) Bellefeuille, J. A.; Grapperhaus, C. A.; Buonomo, R. M.; Reibenspies, J. H.; Darensbourg, M. Y. *Organometallics* **1998**, *17*, 4813–4821.
(61) Gainsford, G. J.; Jackson, W. G.; Sargeson, A. M. *J. Am. Chem. Soc.* **1982**, *104*, 137–141.
(62) Schenck, W. A.; Frisch, J.; Adam, W.; Prechtl, F. *Inorg. Chem.* **1992**, *31*, 3329–3331.
(63) Gildersleeve, J.; Rascal, R. A.; Kahne, D. *J. Am. Chem. Soc.* **1998**, *120*, 5961–5969.
(64) Noble, M. E. *Inorg. Chem.* **1990**, *29*, 1337–1342.
(65) Lee, J. Q.; Sampson, M. L.; Richardson, J. F.; Noble, M. E. *Inorg. Chem.* **1995**, *34*, 5055–5064.
(66) Martinsen, A.; Songstad, J. *Acta Chem. Scand. A* **1977**, *31*, 645–650.

causing the color to go very dark. The solution was removed from the ice bath. Additional H_2O (10 mL) was added dropwise, and the slurry was stirred for 5 min and then filtered. The solid was washed (1:2 Me_2CO/H_2O) and then suction-dried to give an olive solid (0.3662 g, 99% crude yield). The ^{31}P NMR spectrum revealed 96 mol % purity.

Crude product (0.3510 g) and silica gel (3.5113 g) were stirred together for several minutes in 15 mL of CH_2Cl_2, and the mixture was then filtered. The silica gel fraction was washed with CH_2Cl_2 (25 mL). The orange silica gel fraction, without drying, was then washed slowly and in several portions with a total of 38 mL of Me_2CO; this released the product, giving an olive filtrate and a pale yellow silica remainder. The olive filtrate was rotavapped. The residue was promptly dissolved in 8.0 mL of EtOH, and this solution was treated slowly with 8.0 mL of H_2O. Filtration and washing yielded very dark crystals of **1** (0.2983 g, 84% calcd overall yield). The compound was typically stored at freezer temperatures of −15 °C or so.

BnS{Mo_2}SOMe$^+CF_3SO_3^-$, 4$^+$(Me)$CF_3SO_3^-$. In a glovebag under N_2, BnS{Mo_2}SO, **1** (0.1611 g, 0.1606 mmol) was dissolved in 1.5 mL of dry CH_2Cl_2. To this olive solution was added CF_3SO_3Me (20 μL, 0.18 mmol), quickly lightening the color. The stoppered flask was removed from the glovebag, and the solution was stirred for 4 min to give a yellow−orange solution. After opening to the air, the solution was rotavapped. The residue was dissolved in 1.2 mL of EtOH, and then 2.4 mL of H_2O were added. The slurry was stirred for 1.4 h and filtered. The product was washed (1:3 EtOH/H_2O) and suction-dried to give a yellow powder (0.1775 g, 95%). ^{31}P NMR (ppm): (109.9 C), (109.7 B), 109.1 (A). ^1H NMR (ppm): 7.65 d (A), (7.60 d), 7.55 t (A), 7.47 t (A), Bn−H; (6.82 br), (6.74 br), (6.65 d), 6.62 d (A), 6.58 d (A), To−H; (4.79 s, C), 3.96 s (A), (3.61 s, B), Bn−CH_2; (4.37 s, B), 4.23 s (A), $SOCH_3$; 4.26 m, 4.07 dq, $POCH_2$; (2.21 s), 2.13 s (A), To−CH_3; 1.52 s (A), (1.47 s), O_2CCH_3; 1.44 t (A), 1.24 t (A), $POCCH_3$. Invertomer distribution: 76% A, 16% B, 9% C.

BnS{Mo_2}SOEt$^+CF_3SO_3^-$, 4$^+$(Et)$CF_3SO_3^-$. The reaction steps followed those for **4**$^+$(Me)$CF_3SO_3^-$ above, using **1** (0.1049 g, 0.1046 mmol) and CF_3SO_3Et (15 μL, 0.12 mmol) in 1.5 mL of dry CH_2Cl_2. After the reaction and then rotavapping, Et_2O (2.0 mL) and pet ether (1.5 mL) were added, and this mixture was then stirred for 1.5 h. The slurry was filtered, and the product was then washed (3:2 Et_2O/pet ether) and suction-dried to give a yellow powder (0.1109 g, 90%). ^{31}P NMR (ppm): (110.0 C), (109.7 B), 109.2 (A). ^1H NMR (ppm): 7.65 d (A), (7.60 d), 7.55 t (A), 7.47 t (A), Bn−H; (6.80 br), (6.74 br), (6.65 d), 6.61 d (A), 6.57 d (A), To−H; (4.77 s, C), 3.96 s (A), (3.61 s, B), Bn−CH_2; (4.57 q, B), 4.47 q (A), $SOCH_2$; 4.25 m, 4.07 dq, $POCH_2$; (2.21 s, C), (2.14 s, B), 2.13 s (A), To−CH_3; (1.64 t, B), 1.50 t (A), $SOCCH_3$; 1.50 s (A), O_2CCH_3; 1.43 t (A), 1.24 t (A), $POCCH_3$. Invertomer distribution: 75% A, 16% B, 9% C.

S{Mo_2}SOMe, 5(Me). PPN^+I^- (0.0641 g, 0.0963 mmol) was added to a solution of BnS{Mo_2}SOMe$^+CF_3SO_3^-$ (**4**$^+$(Me)$CF_3SO_3^-$, 0.0936 g, 0.0793 mmol) in Me_2CO (0.9 mL) plus THF (0.6 mL). Through 4 min of stirring, the PPN^+I^- dissolved, and the solution turned red−orange. Then, 1:1 EtOH/H_2O (3.0 mL) was added. The slurry was filtered; the solid was washed (2:1 EtOH/H_2O) and suction-dried to give a red−orange, crystalline product (0.0536 g, 72%). ^{31}P NMR (ppm): 114.9, (114.8). ^1H NMR (ppm): 6.57 d, 6.47 d, To−H; 4.19 m, 4.07 m, $POCH_2$; 3.95 s, $SOCH_3$; 2.08 s, To−CH_3; 1.33 t, 1.21 t, $POCCH_3$; 1.28 s, (1.18 s), O_2CCH_3. Invertomer ratio: 18.

S{Mo_2}SOEt, 5(Et). The synthesis followed that of **5**(Me) above, using **4**$^+$(Et)$CF_3SO_3^-$ (0.1775 g, 0.150 mmol) in Me_2CO (1.0 mL) plus THF (1.0 mL) and PPN^+I^- (0.1204 g, 0.181 mmol), stirring for 5 min. Precipitation with 1:1 EtOH/H_2O (4 mL), followed by filtration, washing (2:1 EtOH/H_2O), and drying, gave a red−orange solid (0.0878 g, 62%). ^{31}P NMR (ppm): 115.0, (114.8). ^1H NMR (ppm): (6.60 d), 6.56 d, 6.46 d (6.45 d), To−H; (4.33 q), 4.20 q, $SOCH_2$; 4.18 m, 4.08 m, $POCH_2$; (2.08 s), 2.08 s, To−CH_3; (1.36 t), 1.36 t, $SOCCH_3$; 1.32 t, (1.22 t), 1.21 t, $POCCH_3$; 1.25 s, (1.18 s), O_2CCH_3. Invertomer ratio: 3.8.

S{Mo_2}SOBn, 5(Bn). To a solution of BnS{Mo_2}SO, **1** (0.0996 g, 0.0993 mmol) in 2 mL of Me_2CO was added BnBr (47 μL, 0.40 mmol). The solution was stirred for 2.9 h. Precipitation using 1:1 EtOH/H_2O (6 mL), followed by filtration, washing (1:1 EtOH/H_2O), and suction-drying, gave an orange powder (0.0570 g, 57%). ^{31}P NMR (ppm): 114.9, (114.8). ^1H NMR (ppm): 7.46 d, 7.29−7.39 m, BnH; 6.54 d, (6.53 d), 6.45 d, (6.32 d), To−H; (5.24 s), 5.14 s, Bn−CH_2; 4.19 dq, 4.09 m, $POCH_2$; 2.08 s, (2.05 s), To−CH_3; 1.32 t, (1.23 t), 1.22 t, $POCCH_3$; (1.17 s), 1.04 s, O_2CCH_3. Invertomer ratio: 3.9.

BnS{Mo_2(P=O)}SOEt, 6. Dark olive BnS{Mo_2}SO, **1** (0.1215 g, 0.121 mmol) was placed into the bottom of a tared tube of dimensions ~16 × 200 mm. The bottom portion of the tube was immersed into a boiling water bath for 150 min. The tube was then briefly immersed in water at room temperature and then dried. The product was an orange−brown solid (0.1207 g, 99%), which was 97 mol % by its ^{31}P NMR spectrum.

Crude product (0.0926 g) was combined with silica gel (1.39 g) in CH_2Cl_2 (4.6 mL) and stirred briefly. The slurry was filtered, and the silica gel fraction was washed with CH_2Cl_2 and then suction-dried. This was washed in portions with 20 mL (total) of Me_2CO, and the combined filtrates were then rotavapped. The residue was dissolved in diglyme (1.2 mL). The addition of H_2O (1.8 mL) and stirring for 2.0 h gave a slurry which was then filtered. Washing (1:2 EtOH/H_2O) and suction-drying gave a yellow powder (0.0710 g, 77% recovery). A trace impurity (~0.5 mol %) remained in the ^{31}P NMR spectrum, while some diglyme (~1 mol %) lingered in the ^1H NMR spectrum. ^{31}P NMR (ppm): (112.2), 111.8 (J_{PP} = 1.5 Hz), $(EtO)_2P$; (76.5), 76.3, (EtO)(O)P. ^1H NMR (ppm): 7.75 d, (7.70, d), 7.50 t, 7.40 t, Bn−H; (6.63 d), 6.55 d, 6.48 d, 6.47 d, 6.39 d, To−H; 4.47 dq, 4.36 dq, $SOCH_2$; 4.23 dq, 4.03 dq, $P(OCH_2)_2$; 4.18 d, 3.81 d, (3.47 d), Bn−CH_2; 3.83 dq, $PO(OCH_2)$; (2.10 s), 2.09 s, (2.05 s), 2.03 s, To−CH_3; (1.53 t), 1.41 t, $SOCCH_3$; 1.43 s, O_2CH_3; 1.39 t, 1.21 t, $P(OCCH_3)_2$; 1.02 t, (1.02 t), $PO(OCCH_3)$. Invertomer ratio: 5.

X-Ray Crystallography. The crystal for the proximal isomer of **5**(Et) was mounted on a glass fiber, while the crystals for the other structures were mounted on a CryoLoop with Paratone oil. Data were collected on a Bruker SMART APEX CCD diffractometer using monochromated Mo Kα radiation. The SMART software package (v. 5.632) was used for data collection. Frame data were processed using SAINT (v. 6.45a); raw *hkl* data were corrected for absorption using SADABS (v. 2.10). The structures were solved by Patterson methods using SHELXS-90 and refined by least-squares methods on F^2 using SHELXL-99 incorporated into the SHELXTL (v. 6.14) suite of programs. Information specific to each structure is given below and summarized in Table 3. More extensive information is given in the Supporting Information. Crystallographic data for the structural analyses have also been deposited with the Cambridge Crystallographic Data Centre (CCDC), and those numbers are given for each structure below.

Crystals of BnS{Mo_2}SOEt$^+CF_3SO_3^-$ (**4**$^+$(Et)$CF_3SO_3^-$) were obtained from layering *n*-C_7H_{16} onto a solution in $MeCCl_3$. The carbon atoms of one dithiophosphate OEt group were modeled with a 50% disorder (C23a−C24a and C23b−C24b) as was the methyl atom (C20a and C20b) of another OEt group. The triflate anion was disordered but was accurately modeled using two half-occupancy fluorine groups (F1a−F3a, and F1b−F3b) and two half-occupancy oxygen groups (O10a−O12a, and O10b−O12b); the carbon and sulfur of the anion were full-occupancy. All non-hydrogen atoms except those involved in set b of the disordered anion were refined anisotro-

Table 3. Selected Crystal Data and Refinement Results

	BnS{Mo_2}SOEt$^+$ (**4**$^+$) $CF_3SO_3^-$	S{Mo_2}SOEt (**5**), distal	S{Mo_2}SOEt (**5**), proximal	BnS{Mo_2(P=O)}SOEt (**6**)
formula	$C_{34}H_{49}F_3Mo_2N_2O_{10}P_2S_7$	$C_{26}H_{42}Mo_2N_2O_7P_2S_6$	$C_{26}H_{42}Mo_2N_2O_7P_2S_6$	$C_{31}H_{44}Mo_2N_2O_7P_2S_6$
fw	1180.99	940.80	940.80	1002.86
T, °C	−173	25	−173	−173
wavelength, Å	0.71073	0.71073	0.71073	0.71073
cryst syst	monoclinic	monoclinic	monoclinic	monoclinic
space group	Cc	$P2_1/c$	$P2_1/c$	$P2_1/n$
a, Å	18.917(4)	17.668(4)	20.448(2)	12.940(3)
b, Å	10.906(2)	9.900(2)	19.771(2)	13.775(3)
c, Å	24.231(4)	23.167(5)	9.470(1)	23.200(5)
β, deg	104.856(4)	90.073(4)	97.819(2)	94.521(4)
V, Å^3	4832.0(15)	4052.1(14)	3792.8(7)	4122.6(14)
D_{calcd}, g/cm^3	1.623	1.542	1.648	1.616
Z	4	4	4	4
abs coeff, mm^{-1}	0.951	1.047	1.118	1.035
cryst size, mm^3	0.25 × 0.20 × 0.02	0.30 × 0.10 × 0.05	0.35 × 0.25 × 0.15	0.29 × 0.22 × 0.08
cryst habit	yellow plate	red-orange needle	orange rhomb prism	orange plate
abs corrn	SADABS	SADABS	SADABS	SADABS
max/min transmission	0.989/0.725	0.941/0.673	0.895/0.733	0.914/0.787
final R_1 ($I > 2\sigma(I)$)[a]	0.0505	0.0455	0.0510	0.0355
final wR_2 ($I > 2\sigma(I)$)[b]	0.1175	0.0857	0.1085	0.0753
GOF[c]	1.03	1.03	1.06	1.02

[a] $R_1 = \sum||F_o| - |F_c||/\sum|F_o|$. [b] $wR_2 = \{\sum[w(F_o^2 - F_c^2)^2]/\sum[w(F_o^2)^2]\}^{1/2}$, where $w = q/\sigma^2(F_o^2) + (qp)^2 + bp$. [c] GOF $= S = \{\sum[w(F_o^2 - F_c^2)^2]/(n-p)\}^{1/2}$.

pically. Hydrogen atoms were placed in their geometrically generated positions and refined as a riding model. Methyl H's were included as fixed contributions with $U(H) = 1.5 \times U_{eq}$ (attached C atom), while the torsion angle which defines its orientation was allowed to refine on the attached C atom. Methylene and phenyl H's were included as fixed contributions with $U(H) = 1.2 \times U_{eq}$ (attached C atom). For all 9175 unique reflections (R(int) = 0.045), the final anisotropic, full matrix least-squares refinement on F^2 for 455 variables converged at (for $I > 2\sigma(I)$) $R_1 = 0.0505$ and $wR_2 = 0.1175$ with a GOF of 1.03 (CCDC No. 710480).

Crystals of distal S{Mo_2}SOEt, **5**(Et), were obtained from layering a solution in MeCN onto H_2O. The disorder in a dithiophosphate OEt group was modeled using two sets of 50% occupancy carbon atoms (C21a−C22a and C21b−C22b). All other non-hydrogen atoms were refined anisotropically. Hydrogen atoms were placed in their geometrically generated positions and refined as a riding model as described above for **4**$^+$(Et)$CF_3SO_3^-$. For all 7235 unique reflections (R(int) = 0.047), the final anisotropic, full matrix least-squares refinement on F^2 for 455 variables converged at (for $I > 2\sigma(I)$) $R_1 = 0.0455$ and $wR_2 = 0.0857$ with a GOF of 1.03 (CCDC No. 710482).

Crystals of proximal S{Mo_2}SOEt, **5**(Et), were obtained from layering EtOH onto a solution in 1,2,3-trichloropropane. The disordered dithiophosphate OEt group was modeled using two sets of carbon atoms; C19a−C20a were refined anisotropically at 80% occupancy and C19b−C20b isotropically at 20%. All non-hydrogen atoms were refined anisotropically. All hydrogen atoms attached to parent carbon atoms were positioned geometrically (C−H = 0.95−0.99 A) and refined using a riding model as described above for **4**$^+$(Et)$CF_3SO_3^-$. For all 8687 unique reflections (R(int) = 0.043), the final anisotropic, full matrix least-squares refinement on F^2 for 423 variables converged at (for $I > 2\sigma(I)$) $R_1 = 0.0510$ and $wR_2 = 0.1085$ with a GOF of 1.06 (CCDC No. 710481).

Crystals of BnS{Mo_2(P=O)}SOEt, **6**, were obtained by storing a test tube containing a solution in Et_2O inside a closed jar with a layer of n-$C_{12}H_{26}$ in the bottom of the jar. All non-hydrogen atoms were refined anisotropically. Hydrogen atoms were placed in their geometrically generated positions and refined as a riding model as described above for **4**$^+$(Et)$CF_3SO_3^-$. For all 7717 unique reflections (R(int) = 0.045), the final anisotropic, full matrix least-squares refinement on F^2 for 422 variables converged at (for $I > 2\sigma(I)$) $R_1 = 0.0355$ and $wR_2 = 0.0753$ with a GOF of 1.02 (CCDC No. 710483).

Acknowledgment. This work was supported in part by the Office of the Vice President for Research at the University of Louisville. M.S.M. thanks the Kentucky Research Challenge Trust Fund for an upgrade of the X-ray facilities.

Supporting Information Available: Additional crystallographic refinement details and data, including CIF files. This material is available free of charge via the Internet at http://pubs.acs.org.